

# Recent cross-section measurements of neutron-induced reactions of importance for background estimates in $0\nu\beta\beta$ searches

W. Tornow<sup>1,2,a</sup>, M. Bhike<sup>1,2</sup>, S.W. Finch<sup>1,2</sup>, and Krishichayan<sup>1,2</sup>

<sup>1</sup> Department of Physics, Duke University, Durham, North Carolina 27708, USA

<sup>2</sup> Triangle Universities Nuclear Laboratory, Durham, North Carolina 27708, USA

**Abstract.** We report on cross-section measurements for the reactions  ${}^{76}\text{Ge}(n,2n){}^{75}\text{Ge}$ ,  ${}^{76}\text{Ge}(n,n'\gamma){}^{76}\text{Ge}$ ,  ${}^{126,127,128}\text{Te}(n,\gamma){}^{127,129,131}\text{Te}$ , and  ${}^{136}\text{Xe}(n,n'\gamma){}^{136}\text{Xe}$  in the neutron energy range between 0.5 MeV and 15 MeV.

## 1. Introduction

Neutron-induced background reactions are a major concern for the next generation of zero-neutrino double-beta decay ( $0\nu\beta\beta$ ), dark-matter and supernova neutrino detectors. There are three sources of neutrons in underground facilities: muon-induced spallation neutrons, neutrons from ( $\alpha,n$ ) reactions and to a lesser extent also neutrons from the spontaneous fission of  ${}^{238}\text{U}$ . The primary spallation neutron energy spectrum could extend up to a few GeV. These neutrons slow down in the rock, mainly due to ( $n,xn$ ) reactions with  $x \geq 2$ , generating a neutron shower at the detector location. Active neutron and muon shielding is commonly used to reduce or eliminate possible neutron-induced background events by tagging the associated muon in a veto counter surrounding the detector, and by rejecting any events from the data analysis for a certain time interval after muon detection. Furthermore, the muon veto detector itself acts as a neutron veto. Therefore, spallation neutrons are not considered to create the dominant contribution to the neutron-induced background, unless the neutron veto efficiency is below 95%, which is normally the case only for incident neutron energies below 5 MeV. Here, we assume a muon veto efficiency of 99%. Isotopes from the thorium and uranium decay chains provide a source of  $\alpha$ -particles which could interact with low and medium mass nuclei to initiate the ( $\alpha,n$ ) reaction, resulting in neutrons with energies up to approximately 10 MeV. These neutrons, if created outside of the fiducial volume of the detector or within its shielding are difficult to deal with due to the lack of effective tagging possibilities. The same is true for neutrons from the spontaneous fission of  ${}^{238}\text{U}$ , although their yield is smaller than that of the ( $\alpha,n$ ) neutrons. Like the ( $\alpha,n$ ) neutrons, their energy spectrum extends up to about 10 MeV. Therefore, actinide impurities in the detector medium itself and its surrounding shielding produce neutrons with energies up to 10 MeV. These are the ones that could escape tagging or vetoing and therefore

have the potential to induce reactions within the detector which could mimic the  $0\nu\beta\beta$  decay signal of interest.

In order to estimate the level of neutron-induced background events in  $0\nu\beta\beta$  searches, the relevant neutron cross-section data of the detector and shielding materials are needed in the neutron energy range up to approximately 10 MeV. Here, we report on our experimental studies, focusing on the  $0\nu\beta\beta$  decay nuclei  ${}^{76}\text{Ge}$ ,  ${}^{130}\text{Te}$  and  ${}^{136}\text{Xe}$ . However, because in practice the associated detectors do not consist to 100% of the isotope of interest, neutron-induced cross-section data are also needed for  ${}^{74}\text{Ge}$ ,  ${}^{126,128}\text{Te}$ , and  ${}^{134}\text{Xe}$ .

Returning to the ( $n,xn$ ) reactions we note that these reactions are the most powerful process in slowing down medium energy neutrons until their energy approaches approximately 8 MeV. The resulting nuclei are often radioactive and the decay  $\gamma$  rays are a potential source of unwanted background in many rare decay searches. Below 8 MeV, the ( $n,2n$ ) channel is not open anymore and inelastic neutron scattering, i.e., the ( $n,n'\gamma$ ) reaction and the radiative neutron capture reaction ( $n,\gamma$ ) are the most important sources of  $\gamma$ -ray background. Below approximately 2.5 MeV neutron energy, the ( $n,\gamma$ ) reaction becomes the sole source of  $\gamma$ -ray background in  $0\nu\beta\beta$  searches. In contrast to neutron inelastic scattering, the capture process produces much higher energy  $\gamma$  rays (up to the neutron binding energy plus the neutron kinetic energy). The de-excitation  $\gamma$  rays are often prompt, but if the ground state is radioactive and decays, for example, via  $\beta$ -decay, then delayed radiation is produced, which is often more difficult to deal with than is the case with prompt events, where tagging possibilities may exist. Of course, if the  $\beta$ -decay Q-value is smaller than about 2.5 MeV, the possible energy sum is below the energy region of interest.

## 2. Experimental procedure

The experiments are being performed at the Triangle Universities Nuclear Laboratory (TUNL), located on the campus of Duke University. Mono-energetic neutrons are produced via the  ${}^7\text{Li}(p,n){}^7\text{Be}$ ,  ${}^3\text{H}(p,n){}^3\text{He}$ ,  ${}^2\text{H}(d,n){}^3\text{He}$ ,

<sup>a</sup> e-mail: [tornow@tunl.duke.edu](mailto:tornow@tunl.duke.edu)

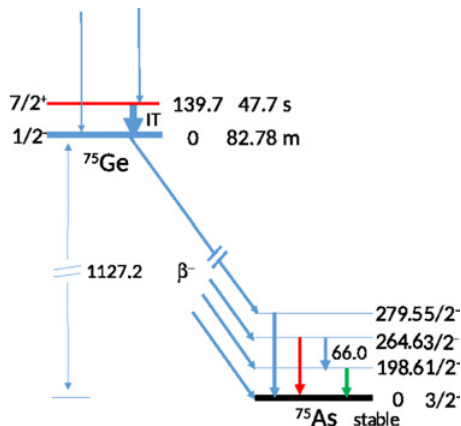


**Figure 1.** Partial level scheme relevant to the  $^{76}\text{Ge}(n,2n)^{75m}\text{Ge}$  and  $^{76}\text{Ge}(n,2n)^{75}\text{Ge}$  reactions. All energies are given in keV. Data taken from [4].

and  $^3\text{H}(d,n)^4\text{He}$  reactions. The charged-particle beams are delivered and accelerated at TUNL's tandem accelerator facility.

The well-established neutron activation technique is used. After irradiation, the samples and associated monitor foils needed for neutron fluence determination are  $\gamma$ -ray counted in TUNL's low-background counting facility with HPGe detectors of 55% and 60% relative efficiency. The absolute photo-peak efficiency of these detectors is measured using a series of calibrated  $\gamma$ -ray test sources. Standard data-acquisition systems and software are used to accumulate and analyze the spectra.

The activation formula is used twice. First, for determining the neutron flux at the sample position from the measured activity of the monitor foils and the known cross section for the reaction of interest. Second, using this information, the activation formula is used again, this time with the measured activity of the irradiated sample to determine the cross section of interest. Monte-Carlo simulations are used to account for the different size of the  $\gamma$ -ray test sources and the various samples studies in the present work.

### 3. Results

#### 3.1. $^{76}\text{Ge}(n,2n)^{75}\text{Ge}$ reaction

The GERDA [1] and MAJORANA [2] collaborations use HPGe detectors as both source and target in their searches for the  $0\nu\beta\beta$  decay of  $^{76}\text{Ge}$ . These HPGe detectors are enriched to approximately 86% in  $^{76}\text{Ge}$  and 14% in  $^{74}\text{Ge}$ . The Q-value for  $0\nu\beta\beta$  of  $^{76}\text{Ge}$  is  $Q = 2039.0\text{ keV}$ . Therefore, neutron-induced reactions on these two isotopes are a concern, if  $\gamma$  rays with energies in the 5 keV wide window centered at the Q-value of  $0\nu\beta\beta$  are produced. As stated in the introduction, the (n,2n) reaction with its large cross section plays a dominant role in the slowing-down process of muon-induced spallation neutrons. Therefore, its cross section is needed for accurately tracing neutrons in the planned 1-tonne  $^{76}\text{Ge}$   $0\nu\beta\beta$  detector. The (n,2n) reaction on  $^{76}\text{Ge}$  leaves the daughter nucleus  $^{75}\text{Ge}$  in either the isomeric state at 139.7 keV excitation energy or the ground state, which in turn decays via  $\beta$ -decay to the stable  $^{75}\text{As}$  nucleus (see Fig. 1). The half-life times of  $^{75}\text{Ge}$  are suitable or

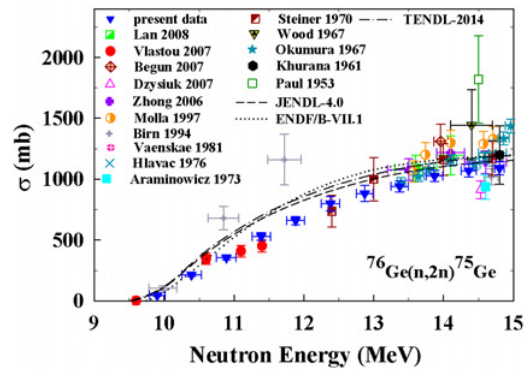


**Figure 2.** Cross-section results for the  $^{76}\text{Ge}(n,2n)^{75}\text{Ge}$  reaction compared with results from earlier measurements and the evaluations TENDL-2014, JENDL-4.0 and ENDF/B-VII.1.

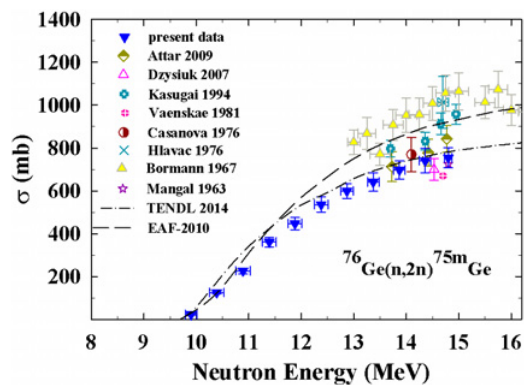


**Figure 3.** Experimental results for  $^{76}\text{Ge}(n,2n)^{75m}\text{Ge}$  reaction compared with results from earlier measurements and the evaluations TENDL-2014 and EAF-2010.

the activation technique, although the short half-life of the isomeric state of  $T_{1/2} = 47.7\text{ s}$  makes the measurements quite demanding. The decay of  $^{75}\text{Ge}$  will not produce any delayed decay products with energy sum at or above 2039.0 keV.

In Figs. 2 and 3 the downside pointing triangles represent our measured  $^{76}\text{Ge}(n,2n)^{75}\text{Ge}$  ground-state and  $^{76}\text{Ge}(n,2n)^{75m}\text{Ge}$  isomeric-state transition cross sections in comparison to existing data and evaluations and the model calculation TENDL-2014 based on the TALYS code [3]. As can be seen in Fig. 2, our data are in good agreement with the few previously existing data below 13 MeV. In the heavily researched energy range centered at 14 MeV neutron energy, our data support the lower band of data, while the evaluations and model calculations try to reproduce the average of the existing data in this energy region, resulting in an overrepresentation of the cross section at lower energies. Figure 3 shows that previous data for the isomeric cross section exist only in the 14 MeV energy region. Again, our data are in good agreement with the lower band of the existing data. We note that the TENDL-2014 model calculation is in better agreement with our data for the isomeric cross section than for the ground-state cross section, while the EAF evaluation reproduces the average of the previously existing data. Finally, we point out that the ground-state and isomeric-state (n,2n) cross sections for  $^{76}\text{Ge}$  are of similar magnitude.

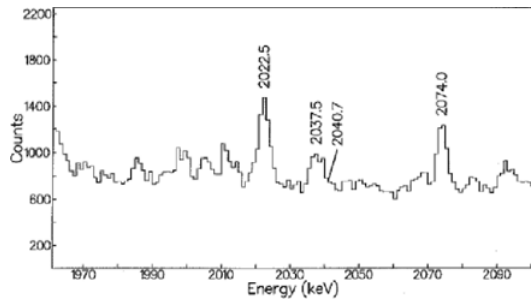


**Figure 4.** Pulse-height spectrum for  $^{76}\text{Ge}(n,n'\gamma)^{76}\text{Ge}$  at  $E_n=5$  MeV.

Before moving on to the next reaction, we note that the activation technique cannot be applied to measure the  $^{74}\text{Ge}(n,2n)^{73}\text{Ge}$  cross section because  $^{73}\text{Ge}$  is stable.

### 3.2. $^{76}\text{Ge}(n,n'\gamma)^{76}\text{Ge}$ reaction

Inelastic neutron scattering to levels which coincide with the Q-value of  $0\nu\beta\beta$  decay candidates is a major concern, especially if there is a sizeable branching ratio for a single  $\gamma$ -ray transition to the ground state. Gamma-ray cascades to the ground state may be recognized by pulse-height digitizers as multi-site events and subsequently could be rejected, unless one or more of the associated  $\gamma$  rays do not interact within the detector. In contrast, the  $0\nu\beta\beta$  signal of interest is a single-site event, created by two  $\beta$  particles of short range in the detector. The early work of Camp and Foster [5], which forms the basis of the level scheme of  $^{76}\text{Ge}$ , shows a state at 3951.9 keV which decays to the 1911.1 keV level, resulting in the emission of a 2040.7 keV  $\gamma$  ray, in close proximity to the 2039.0 keV Q-value of  $^{76}\text{Ge}$  (see Fig. 5). Recently, this level and its decay properties were confirmed in Ref. [6], using the  $^{76}\text{Ge}(n,p)^{76}\text{Ga}$  reaction, as in the original work of Ref. [5]. However, searches by [7] did not reveal the 2040.7 keV  $\gamma$ -ray line. Similarly, the work of Ref. [8] and of our group at lower neutron energies did not result in a positive observation of this transition, although some hints may be present in the  $\gamma$ -ray spectra measured by both groups. However, the spectrum of Ref. [8] clearly show a new  $\gamma$ -ray line at 2037.5 keV, again in close proximity to 2039.0 keV. Figure 4 shows a spectrum obtained by our group with 5 MeV incident neutrons which also shows this peak. Presently, it cannot be ruled out that the peak at 2037.5 keV is not a single line, because it is a bit broader than expected. With some imagination the expected line at 2040.7 keV could be seen in Fig. 4 as a shoulder to the right of the 2037.5 keV peak. Our spectra obtained at 8 and 12 MeV neutron energy are not conclusive either. Currently, there is no agreement on the origin of the 2037.5 keV transition. Coincidence measurements are needed to place this transition into the  $^{76}\text{Ge}$  level scheme. Returning to the 2040.7 keV transition we note that, although not observed, its  $^{76}\text{Ge}(n,n'\gamma)^{76}\text{Ge}$  production cross section can be determined from the measured yield of other observed decay transitions of the 3951.5 keV state, and using the branching ratios of Ref. [5] (see also Fig. 5). Using this approach the cross section for producing the 2040.7 keV transition is estimated to be 10 mb. In comparison, the newly observed

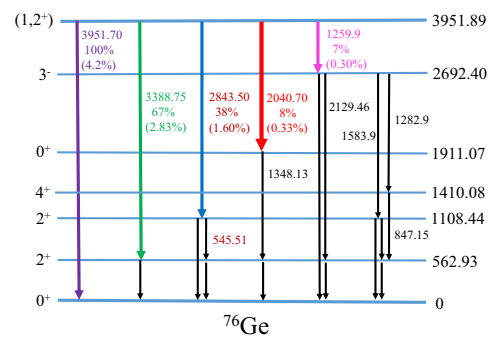


**Figure 5.** Partial level scheme of  $^{76}\text{Ge}$  [4]. The transitions of interest with their branching ratios are given by bold arrows. The branching ratios given in parentheses refer to the decay of  $^{76}\text{Ga}$ . Energies are in keV.

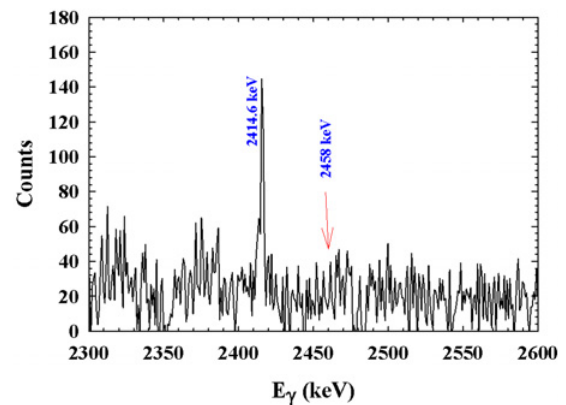


**Figure 6.** Portion of the  $\gamma$ -ray energy spectrum between 2300 and 2600 keV. The expected  $0\nu\beta\beta$  energy of 2458 keV is labeled with an arrow. The spectrum shown is the difference spectrum of a filled  $^{136}\text{Xe}$  sphere and an empty sphere.

2037.5 keV transition must have a cross section of the order of 100 mb at 5 MeV incident neutron energy.

The presently available experimental information on the  $^{74}\text{Ge}(n,n'\gamma)^{74}\text{Ge}$  reaction indicates that there are no transitions with  $\gamma$ -ray energies covering the  $0\nu\beta\beta$  decay Q-value window of  $^{76}\text{Ge}$ . However, like in the case of  $^{76}\text{Ge}$ , detailed experimental information is still lacking for neutron energies in the important 5 to 10 MeV neutron energy window.

### 3.3. $^{136}\text{Xe}(n,n'\gamma)^{136}\text{Xe}$ reaction

The EXO-200 [9] and KamLAND-Zen [10] collaborations use  $^{136}\text{Xe}$  in their searches for the elusive  $0\nu\beta\beta$  decay. The EXO-200 two-phase (liquid-gaseous) time-projection chamber operates with xenon enriched to approximately 81% in  $^{136}\text{Xe}$ , with a remaining 19% contribution of  $^{134}\text{Xe}$ . The KamLAND-Zen detector is based on a liquid scintillator loaded with gaseous xenon composed of approximately 91%  $^{136}\text{Xe}$  and 9%  $^{134}\text{Xe}$ . Therefore,  $(n,n'\gamma)$  data are needed for both  $^{136}\text{Xe}$  and  $^{134}\text{Xe}$ . The Q-value for  $0\nu\beta\beta$  decay of  $^{136}\text{Xe}$  is 2457.8 keV. There are known states in  $^{136}\text{Xe}$  at 2414.6 keV, 2444.39 keV, and 2465.03 keV, all within the energy resolution of the EXO-200 and KamLAND-Zen detectors, but only the 2414.6 keV state has a strong branching ratio to the ground state. This is demonstrated in Fig. 6, where a spectrum obtained with 5 MeV neutrons for the  $^{136}\text{Xe}(n,n'\gamma)^{136}\text{Xe}$

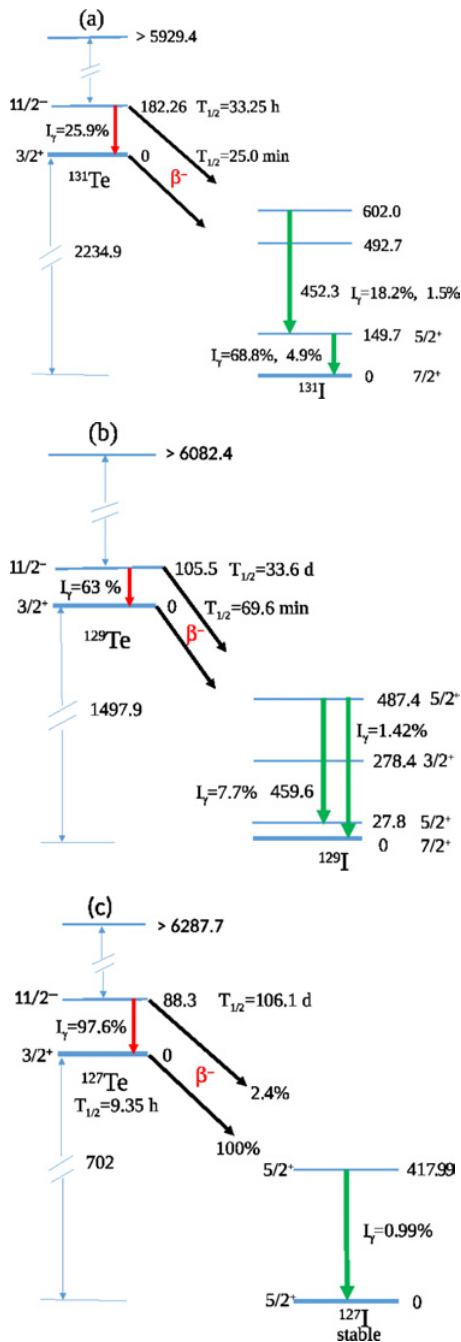


**Figure 7.** Partial nuclear level schemes of importance for (a)  $^{130}\text{Te}(n,\gamma)^{131}\text{Te}$  reaction, (b)  $^{128}\text{Te}(n,\gamma)^{129}\text{Te}$  reaction, and (c)  $^{126}\text{Te}(n,\gamma)^{127}\text{Te}$  reaction.

reaction is presented. It clearly shows the 2414.6 keV  $\gamma$ -ray transition to the ground state of  $^{136}\text{Xe}$ . Data at other neutron energies are needed to determine the energy dependence of its production cross section. Preliminary data are available from our work at 5 and 8 MeV.

A new transition has recently been observed at 2485.6 keV in the reaction  $^{134}\text{Xe}(n,n'\gamma)^{134}\text{Xe}$  by the Kentucky group [11]. Clearly, work is needed to study the  $^{134}\text{Xe}(n,n'\gamma)^{134}\text{Xe}$  reaction in the 5 to 10 MeV energy range, where experimental data do not exist.

### 3.4. $^{126,128,130}\text{Te}(n,\gamma)^{127,129,131}\text{Te}$ reactions

The CUORE collaboration [12] is using natural tellurium (18.8%  $^{126}\text{Te}$ , 31.7%  $^{128}\text{Te}$ , and 34.1%  $^{130}\text{Te}$ ) to search for

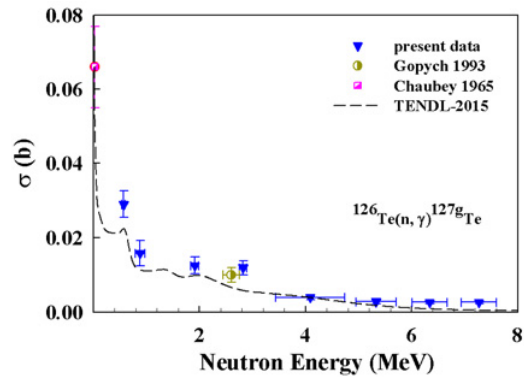


**Figure 8.** Present cross-section results (downward-pointing triangles) for the  $^{126}\text{Te}(n,\gamma)^{127g}\text{Te}$  ground-state reaction in comparison to previous data and the TENDL-2015 model calculation.

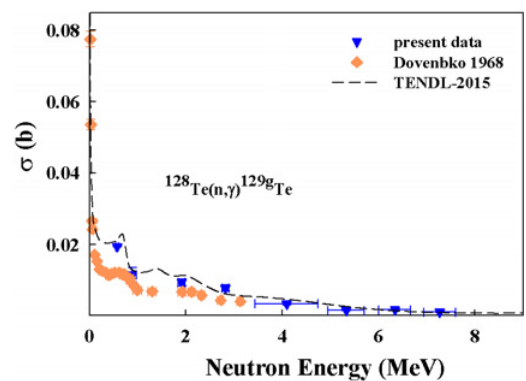


**Figure 9.** Present cross-section results (downward-pointing triangles) for the  $^{128}\text{Te}(n,\gamma)^{129g}\text{Te}$  ground-state reaction in comparison to previous data and the TENDL-2015 model calculation.

the  $0\nu\beta\beta$  decay of  $^{130}\text{Te}$ , employing TeO<sub>2</sub> bolometers. In addition, the SNO+ collaboration [13] is gearing up to reach the same goal, using a liquid scintillator detector loaded with approximately 0.3% (by weight) of a tellurium compound. The Q-value for  $0\nu\beta\beta$  decay of  $^{130}\text{Te}$  is 2527.5 keV. This high Q-value, compared to  $^{76}\text{Ge}$ , makes both  $^{136}\text{Xe}$  and  $^{130}\text{Te}$  very attractive for  $0\nu\beta\beta$  searches, because of the relatively small natural radioactive background at these high energies. Partial level schemes of interest are shown in Fig. 7.

Radiative neutron capture experiments were performed in the neutron energy range between 0.6 MeV and 7.5 MeV for the three tellurium isotopes  $^{126}\text{Te}$ ,  $^{128}\text{Te}$  and  $^{130}\text{Te}$ . For the latter, data were also obtained at 14.8 MeV.

Figure 8 shows our  $^{126}\text{Te}(n,\gamma)^{127g}\text{Te}$  ground-state cross-section data in comparison with the datum of Chaubey et al. [14] at thermal energy and that of Gopych et al. [15] near 2.5 MeV, and the TENDL-2015 model calculation, which provides a reasonably good description of the experimental data. An even better description can be seen in Fig. 9 between our data for the  $^{128}\text{Te}(n,\gamma)^{129g}\text{Te}$  ground-state cross section and the TENDL-2015 prediction. Here, the data of Dovenbko et al. [16] below 3 MeV are lower than our data. Finally, in Fig. 10 our cross-section data for the  $^{130}\text{Te}(n,\gamma)^{131g}\text{Te}$  ground-state and  $^{130}\text{Te}(n,\gamma)^{131m}\text{Te}$  isomeric-state transitions are given, again in comparison



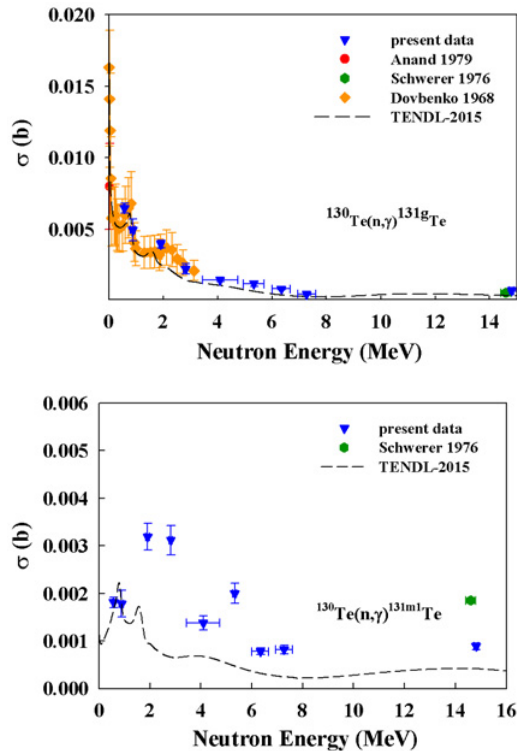


**Figure 10.** Present cross-section results (down pointing triangles) for the  $^{130}\text{Te}(n,\gamma)^{131g}\text{Te}$  ground-state (top) and  $^{130}\text{Te}(n,\gamma)^{131m}\text{Te}$  isomeric-state (bottom) transitions in comparison to previous data and the TENDL-2015 model calculation.

to previous data and the TENDL-2015 model calculation. Our data for the  $^{130}\text{Te}(n,\gamma)^{131g}\text{Te}$  reaction (see Fig. 10 (top)) are in very good agreement with the existing data of Dovenbko et al. [16] below 3 MeV and the single datum of Schwerer et al. [17] near 14.5 MeV, while the TENDL-2015 prediction slightly underestimates the data for energies above 2 MeV. As Fig. 10 (bottom) shows, previous data for the  $^{130}\text{Te}(n,\gamma)^{130m}\text{Te}$  above thermal energies exist only near 14.5 MeV (Schwerer et al. [17]). Our data above 2 MeV follow the trend of the TENDL-2015 prediction, but are higher in magnitude. The datum of Schwerer et al. at 14.8 MeV is even higher than our result.

#### 4. Conclusions

In continuation of our previous work on the reactions  $^{40}\text{Ar}(n,p)^{40}\text{Cl}$  [18],  $^{40}\text{Ar}(n,\gamma)^{41}\text{Ar}$  [19],  $^{74}\text{Ge}(n,\gamma)^{75}\text{Ge}$  [20],  $^{76}\text{Ge}(n,\gamma)^{77}\text{Ge}$  [20],  $^{76}\text{Ge}(n,p)^{76}\text{Ga}$  [6],  $^{76}\text{Ge}(n,2n)^{75}\text{Ge}$  [21],  $^{136}\text{Xe}(n,\gamma)^{137}\text{Xe}$  [22], and  $^{136}\text{Xe}(n,2n)^{135}\text{Xe}$  [23], we present data and their comparison to previously existing data and evaluations and model calculations for the reactions  $^{76}\text{Ge}(n,2n)^{75}\text{Ge}$ ,  $^{76}\text{Ge}(n,n'\gamma)^{76}\text{Ge}$ ,  $^{136}\text{Xe}(n,n'\gamma)^{136}\text{Xe}$ , and  $^{126,128,130}\text{Te}(n,\gamma)^{127,129,131}\text{Te}$ .

This work was supported in part by the US Department of Energy, Office of Nuclear Physics under Grant No. DE-FG02-ER41033.

#### References

- [1] M. Agostini et al., Phys. Rev. Lett. **111**, 122503 (2013)
- [2] M. Abgrall et al., Ad. High Energy Phys. **2014**, 1 (2014)
- [3] A.J. Koning, S. Hilaire and M.C. Duijvestijn, TALYS-1.0'', Proceedings of the International Conference on Nuclear Data for Science and Technology - ND2007, April 22–27, 2007, Nice, France, eds. O. Bersillon, F. Gunsing, E. Bauge, R. Jacqmin and S. Leray, EDP Sciences, 211 (2011)
- [4] <http://www.nndc.bnl.gov/>
- [5] D.C. Camp and B.P. Foster, Nucl. Phys. A **177**, 401 (1971)
- [6] W. Tornow, Megha Bhike, B. Fallin, and Krishichayan, Phys. Rev. C **93**, 014614 (2016)
- [7] C. Rouki, A.R. Domula, J.C. Drohe, A.J. Koning, A.J.M. Plompen, and K. Zuber, Phys. Rev. C **88**, 054613 (2013)
- [8] B.P. Crider, E.E. Peters, J.M. Allmond, M.T. McEllistrem, F.M. Prados-Estévez, T.J. Ross, J.R. Vanhoy, and S.W. Yates, Phys. Rev. C **92**, 034310 (2015)
- [9] J.B. Albert et al., Nature (London) **510**, 229 (2014)
- [10] A. Gando et al., Phys. Rev. Lett. **117**, 082503 (2016)
- [11] E.E. Peters, T.J. Ross, B.P. Crider, S.F. Ashley, A. Chakraborty, M.D. Hennek, A. Kumar, S.H. Liu, M.T. McEllistrem, F.M. Prados-Estévez, J.S. Thrasher, and S.W. Yates, EPJ Web of Conferences **93**, 010207 (2015)
- [12] K. Alfonso et al., Phys. Rev. Lett. **115**, 102502 (2015)
- [13] A. Andringa et al., Journal of Physics: Conference Series **665**, 012080 (2016)
- [14] A.K. Chaubey, and M.L. Sehgal, Nucl. Phys. **66**, 267 (1965)
- [15] P.M. Gopych, I.I. Zalyubovskii, P.S. Kizim, V.I. Sorokin, V.V. Sotnikov, E.A. Fomin, Atom. Ener. **74**, 78 (1993)
- [16] A.G. Dovbenko, E. Kolesov, V.P. Koroleva, and A. Tolstikov, Sov. Atm. Ener. **27**, 1185 (1968)
- [17] O. Schwerer, M. Winkler-Rohatsch, H. Warhanek, and G. Winkler, Nucl. Phys. A, **264**, 105 (1976)
- [18] C. Bhatia, S.W. Finch, M.E. Gooden, and W. Tornow, Phys. Rev. C **86**, 041602(R) (2012)
- [19] Megha Bhike, and W. Tornow, Phys. Lett. B **736**, 741 (2014)
- [20] Megha Bhike, B. Fallin, Krishichayan, and W. Tornow, Phys. Lett. B **741**, 150 (2015)
- [21] Megha Bhike, Krishichayan and W. Tornow, submitted to Phys. Rev. C
- [22] Megha Bhike, and W. Tornow, Phys. Rev. C **89**, 031602 (2014)
- [23] C. Bhatia, S.W. Finch, M.E. Gooden, and W. Tornow, Phys. Rev. C **87**, 011601(R) (2012)